SCIENTIFIC REPORTS

OPEN

SUBJECT AREAS:
SOLID-STATE CHEMISTRY
CHEMICAL PHYSICS
BATTERIES

Received
29 October 2014

Accepted
6 January 2015

Published
28 January 2015

Correspondence and requests for materials should be addressed to H.N. (nisihara@tagen.tohoku.ac.jp)

Li-Rich Li-Si Alloy As A Lithium-Containing Negative Electrode Material Towards High Energy Lithium-Ion Batteries

Shinichiroh Iwamura[1,2], Hirotomo Nishihara[1], Yoshitaka Ono[1], Haruhiko Morito[1], Hisanori Yamane[1], Hiroki Nara[3], Tetsuya Osaka[3] & Takashi Kyotani[1]

[1]Institute of Multidisciplinary Research for Advanced Materials, Tohoku University, 2-1-1 Katahira, Aoba-ku, Sendai, 980-8577, Japan, [2]Division of Chemical Process Engineering, Graduate School of Engineering, Hokkaido University, N13W8 Kita-ku, Sapporo 060-8628, Japan, [3]Faculty of Science and Engineering, Waseda University, 3-4-1, Okubo, Shinjuku-ku, Tokyo, 169-8555, Japan.

Lithium-ion batteries (LIBs) are generally constructed by lithium-including positive electrode materials, such as $LiCoO_2$, and lithium-free negative electrode materials, such as graphite. Recently, lithium-free positive electrode materials, such as sulfur, are gathering great attention from their very high capacities, thereby significantly increasing the energy density of LIBs. Though the lithium-free materials need to be combined with lithium-containing negative electrode materials, the latter has not been well developed yet. In this work, the feasibility of Li-rich Li-Si alloy is examined as a lithium-containing negative electrode material. Li-rich Li-Si alloy is prepared by the melt-solidification of Li and Si metals with the composition of $Li_{21}Si_5$. By repeating delithiation/lithiation cycles, Li-Si particles turn into porous structure, whereas the original particle size remains unchanged. Since Li-Si is free from severe constriction/expansion upon delithiation/lithiation, it shows much better cyclability than Si. The feasibility of the Li-Si alloy is further examined by constructing a full-cell together with a lithium-free positive electrode. Though Li-Si alloy is too active to be mixed with binder polymers, the coating with carbon-black powder by physical mixing is found to prevent the undesirable reactions of Li-Si alloy with binder polymers, and thus enables the construction of a more practical electrochemical cell.

Lithium-ion batteries (LIBs) are widely used for various mobile electronics[1–3], but their energy density is required to be increased further especially for automobile applications such as electric vehicles. The development of new electrode materials having large capacities are of great interest in recent years[4]. For example, silicon (Si) has an extremely large theoretical capacity of 3572 mAh g^{-1} (as $Li_{15}Si_4$)[5–6] as a negative-electrode material, compared to conventional graphite (theoretical capacity is 372 mAh g^{-1}), and Si-containing negative-electrode materials with excellent performances have been intensively developed[7–20]. It should be, however, noted that the energy density of a LIB cell (W_{cell}) depends both on negative- and positive-electrode capacities[21], i.e., a very large negative-electrode capacity does not always result in a significant increase of W_{cell} without the increase of a positive-electrode capacity at the same time. This could be easily understood from Fig. 1, where W_{cell} is plotted against a negative-electrode capacity (based on the construction of a common cylindrical 18650 cell). The present LIBs are generally constructed by graphite (372 mAh g^{-1}) and $LiCoO_2$ (140 mAh g^{-1}) and this combination produces a cell voltage of 3.7 V, so that the value of W_{cell} can be calculated to be about 188 Wh kg^{-1} (See the calculation details in the Supporting Information). As long as $LiCoO_2$ is used as a positive electrode, its W_{cell} levels off around 250 Wh kg^{-1}, even if the capacity of a negative electrode is increased much more than that of graphite (Fig. 1). There are several candidates for positive electrode materials, such as lithium nickel manganese cobalt oxide, lithium iron phosphate, lithium manganese oxide, and lithium titanate, but their effective capacities are no more than ca. 220 mAh g^{-1} [22–23]. Thus, as long as using these lithium-containing materials as a positive electrode, it is intrinsically unable to significantly improve the energy density of LIBs. Recently, lithium-free positive-electrode materials have attracted great interests from their very high capacities: for example, metal fluorides[24] and sulfur (S)[25–27] have theoretical capacities of 600 and 1672 mAh g^{-1}, respectively. In order to use such lithium-free positive-electrode materials, however, it is necessary for a negative-electrode material to contain lithium beforehand. At a laboratory level, it is common to use Li foil as a counter of the lithium-free positive electrode materials. However, Li foil has a problem of dendrite growth during charge/discharge, and it is difficult

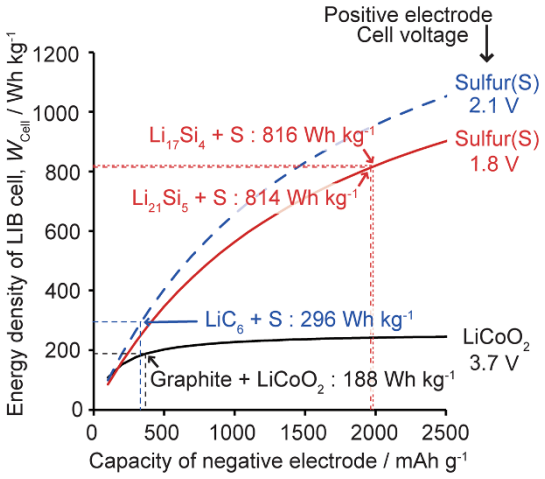

Figure 1 | Energy density of a LIB cell versus capacity of a negative-electrode material. Three lines are calculated with assuming different positive-electrode materials considering their different operating potentials; $LiCoO_2$ (ca. 140 mAh g^{-1}, 3.7 V), S (1672 mAh g^{-1}, 1.8 V), and S (2.1 V). Details about the calculation are given in the Supporting Information.

to adopt it to commercial LIBs, especially large batteries. Lithiated graphite (LiC_6; theoretical capacity is 339 mAh g^{-1}-LiC_6) can be considered as a probable candidate, because it has been already commercialized in lithium-ion capacitors[28]. With the combination of LiC_6 and S, the operating potential could be 2.1 V, and the energy density of LIB reaches 296 Wh kg^{-1} (Fig. 1). If much higher capacity material could be used, the energy density of LIB would be further increased. An ultimate candidate is Li-Si alloy[29]. One method to prepare Li-Si alloy is electrochemical pre-lithiation of Si like the case of the aforementioned lithiated graphite. However, the pre-lithiation requires complicated cell design and the application to Si would be very difficult because of its severe volume expansion upon the lithiation. Thus, the use of thermochemically-synthesized Li-Si alloy is more favorable. There are several Li-rich stable phases in the Li-Si binary system, such as $Li_{21}Si_5$ (theoretical capacity: 1967 mAh g^{-1}-$Li_{21}Si_5$)[30] and $Li_{17}Si_4$ (theoretical capacity: 1978 mAh g^{-1}-$Li_{17}Si_4$)[31]. With combining S with either $Li_{21}Si_5$ or $Li_{17}Si_4$, very high W_{cell} of 814 or 816 Wh kg^{-1} could be achieved (Fig. 1). Thus, Li-rich Li-Si alloy has a great potential as a lithium-containing negative electrode.

Though there are a lot of reports on electrochemical lithiation of Si to form amorphous Li-Si alloys[21,32] or crystalline $Li_{15}Si_4$[5–6], there have been a limited number of publications on the electrochemical behavior of thermochemically-synthesized Li-Si alloys. Weydanz *et al.* have reported the charge/discharge behavior of Li-Si alloy at room temperature for the first time[33]. They prepared several Li-Si alloys, containing $Li_{12}Si_7$, Li_7Si_3, $Li_{13}Si_4$, or $Li_{21}Si_5$, by mechanical mixing of Si and Li and the subsequent annealing. The Li-richest $Li_{21}Si_5$ showed a delithiation capacity of ca. 470 mAh g^{-1}-$Li_{21}Si_5$ at the 2nd cycle, which is much less than the theoretical capacity of $Li_{21}Si_5$ (1967 mAh g^{-1}-$Li_{21}Si_5$). In addition, its capacity faded to 300 mAh g^{-1}-$Li_{21}Si_5$ as early as 10 cycles. Shigematsu's group has reported the first delithiation and lithiation capacities of $Li_{21}Si_5$ as 650 and 300 mAh g^{-1}-$Li_{21}Si_5$, and it quickly faded down to 37 mAh g^{-1}-$Li_{21}Si_5$ at the 4th cycle[34]. They concluded that Li-Si alloy is too reactive to be used in conventional electrolytes, and they applied Li-Si alloy to all-solid-state lithium batteries[34–35]. Ma *et al.* have synthesized amorphous $Li_{12}Si_7$ by the reaction of Si with LiH and the subsequent ball-milling, and reported its charge/discharge performance[36]. However, they used the amorphous $Li_{12}Si_7$ in the same manner as in the conventional lithium-free negative electrode like Si, *i.e.*, they started from the insertion of Li into $Li_{12}Si_7$, rather than the extraction of Li. Tang *et al.* prepared LiSi (Li : Si = 1 : 1) alloy by highly energetic ball-milling[37]. When it was charged/discharged under a capacity restriction of $x < 1$ in Li_xSi, LiSi exhibited the initial discharge capacity of 870 mAh g^{-1}-Si, corresponding to 698 mAh g^{-1}-LiSi. Thus, the earlier studies have not fully investigated the feasibility of Li-rich Li-Si alloy as a lithium-containing negative electrode, and more importantly, there has been almost no discussion on the feasibility of the pre-synthesized Li-Si alloy as a counter electrode of lithium-free positive electrode, and also on its structure change by charge/discharge cycling. Additionally, the previous works might underestimate the ability of the Li-Si alloy, because Li-Si alloys are very reactive and are easily degraded during cell construction.

In this work, we try to bring out the true ability of Li-Si alloy. A Li-rich alloy is prepared by the melting-solidification method from molten Li-Si mixture having the composition of $Li_{21}Si_5$. First, the basic charge/discharge property of the Li-Si alloy and the effect of its particle size are examined by an improved cell-construction in which the performance of Li-Si alloy is more correctly evaluated than in the previous works[33–35]. Next, the feasibility analysis of Li-Si as a lithium-containing negative electrode is conducted by using a full cell containing a lithium-free positive electrode. Moreover, we demonstrate that the severe reaction between Li-Si and binder polymers can be avoided when Li-Si particles are coated with carbon black powder and such a coating allows the construction of a more practical electrochemical cell using Li-Si alloy as a negative electrode.

Results and Discussion

Li-Si alloy was prepared by solidification of a molten Li-Si mixture having the composition of $Li_{21}Si_5$. The resulting Li-Si alloy and its ball-milled powder were analyzed by X-ray diffraction (XRD) without air exposure by using a home-made sealed sample holder. As shown in Fig. 2a, the as-prepared alloy shows an XRD pattern which agrees with the datum of $Li_{21}Si_5$ in the international centre for diffraction data (ICDD)[30]. Note that Zeilinger *et al.* have recently reported that $Li_{17}Si_4$ ($Li_{4.25}Si$) could be an alternative stable phase of $Li_{21}Si_5$ ($Li_{4.2}Si$) from a precise analysis by single crystal XRD, though the powder XRD pattern of $Li_{17}Si_4$ is fitted very well to the $Li_{21}Si_5$ structure[31]. Since the compositions of these two phases are very close, the present Li-Si alloy might contain $Li_{17}Si_4$. However, it is difficult to distinguish $Li_{21}Si_5$ and $Li_{17}Si_4$ by the powder XRD pattern[31], and it is also not necessary for the purpose of this work, *i.e.*, the investigation of the feasibility of Li-rich Li-Si alloy as a counter material for lithium-free positive electrode materials. Accordingly, this work doesn't focus on the identification of the present crystalline Li-Si alloy. The Li-Si alloy thus obtained was crushed into small particles by ball-milling in an inert atmosphere. Fig. 2b and c show scanning electron microscope (SEM) images of Li-Si powders which were prepared under two different conditions. Note that Li-Si samples were observed by SEM without air exposure with a home-made transfer vessel. The primary particle sizes of these two samples can be estimated about 2–5 μm (Fig. 2b) and 0.2–2 μm (Fig. 2c), respectively. These samples are referred to as $Li_{21}Si_5$(2–5 μm) and $Li_{21}Si_5$(0.2–2 μm), respectively. Upon the ball-milling, the XRD peak intensity is decreased (Fig. 2a) and each of the peaks is broadened, indicating an intense decrease of crystallinity of the Li-Si alloy. Note that no new peaks including oxidized species were detected in Fig. 2a after the milling process.

In the case of lithium-free negative electrode materials such as graphite or silicon, it is common to prepare working electrodes by mixing active materials (powder form) with binder polymers and conductive additives. However, Li-Si alloy is so reactive that it strongly reacts with binder polymers. For example, when the present Li-Si alloy is mixed with polytetrafluoroethylene (PTFE) in an Ar-filled glove-box, sparks come off, and the mixture is degraded as a result. Therefore the previous literatures reported the charge/discharge behavior of $Li_{21}Si_5$ alloy by using a pellet of Li-Si/Cu as a

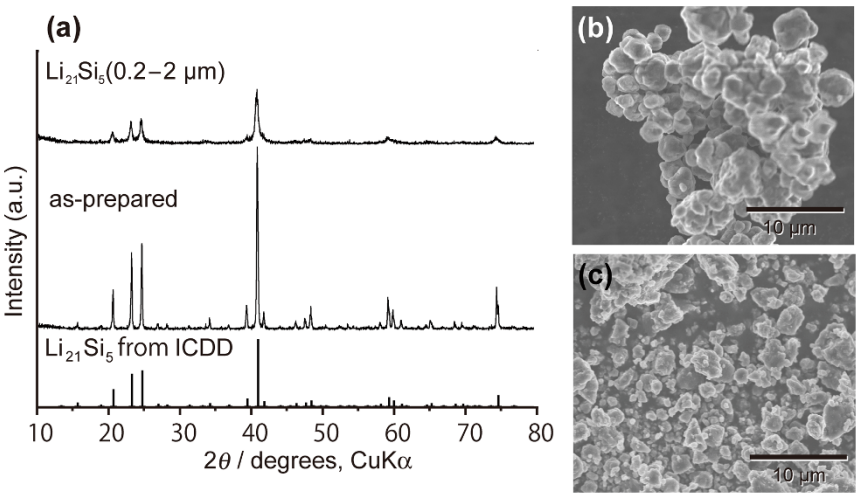

Figure 2 | (a) XRD patterns of as-prepared Li-Si alloy and $Li_{21}Si_5$(0.2–2 μm). The ICDD datum is also shown together[30]. (b,c) SEM images of (b) $Li_{21}Si_5$(2–5 μm) and (b) $Li_{21}Si_5$(0.2–2 μm).

working electrode[33–34]. In these publications, $Li_{21}Si_5$ alloy was mixed with Cu powder in a weight ratio of 1 : 1 and the mixture was pressed into a pellet. It should be noted that the volume ratio of $Li_{21}Si_5$/Cu in a pellet is 7.8 (estimated from the densities of $Li_{21}Si_5$[21] and Cu). Hence, such a small amount of Cu cannot form any continuous current paths, and in addition, the imperfect Cu network could be further destroyed during delithiation/lithiation cycles. Thus, it is very unlikely that the previous researches could realize the full potential of Li-rich Li-Si alloy as a lithium-containing negative electrode. In this work, we decrease the weight ratio of the Li-Si alloy down to 5 wt% (the volume ratio of Li-Si/Cu becomes 0.4). At this composition, Cu powder can form a rigid porous framework and Li-Si alloy is embedded in the resulting porous Cu disk. In a typical procedure, Li-Si alloy was mixed with Cu powders (particle size is ca. 3 μm) and then they were pressed to form a pellet with a diameter of 12 mm and a thickness of 200 μm. During the pressing, the Cu powders are linked each other to form a porous framework, which plays a role of three-dimensional current paths among the Li-Si alloy particles embedded. The pellet thus obtained has a porosity of 21%, so that it can be impregnated with the electrolyte. Then, a three-electrode cell was constructed by using the pellet as a working electrode, and by using two pieces of lithium foil as a counter electrode and a reference electrode, respectively. This electrochemical cell is far from a practical use. Rather, it is aimed purely for a fundamental research. We will discuss a more practical cell construction later.

Charge/discharge cycling was performed in an electrolyte of 1 M $LiPF_6$ in a mixture of ethylene carbonate and diethyl carbonate (1 : 1 by volume). Fig. 3a shows charge/discharge curves of $Li_{21}Si_5$(0.2–2 μm), which is shown in Fig. 2c. In this work, the measurement of Li-Si alloy begins from Li-extraction, an opposite direction of the case of conventional lithium-free negative electrode materials. Since this work aims to evaluate the pre-synthesized Li-Si alloy, its capacity is calculated based on the mass of $Li_{21}Si_5$, which is initially embedded in the working electrode. The initial delithiation is denoted as "pre-delithiation", and from the following lithiation/delithiation, cycle number is counted. The spontaneous potential of Li-Si/Cu electrode was ca. 0.36 V vs. Li/Li^+ and the potential was rapidly increased to 0.45 V as soon as the delithiation started. The spontaneous potential is higher than that of the bulk Li-Si alloy (ca. 0.05 V, see the Supporting Information), probably because of partial delithiation from the Li-Si alloy during the processes of ball-milling, pelletization, and/or constructing the three-electrode cell. Nevertheless, Li-Si alloy samples exhibits an impressive performance in Fig. 3, compared with previous reports on Li-Si alloy[33–34]. $Li_{21}Si_5$(0.2–2 μm) shows a delithiation capacity of 1007 mAh g^{-1} on the basis of the initial active material mass ($Li_{21}Si_5$), in its pre-delithiation process. Accordingly, it is estimated that 51% of lithium is extracted from $Li_{21}Si_5$(0.2–2 μm). The rest of lithium (49%) might remain in the electrode due to partial electrical/ionic isolation, or remain as some irreversible forms, such as oxides/hydroxides. Zhao *et al.* has recently reported that partial oxidation of Li_xSi improves its cyclability[38]. Therefore, the oxidation of Li-Si alloy might not seriously lower its performance. Despite such

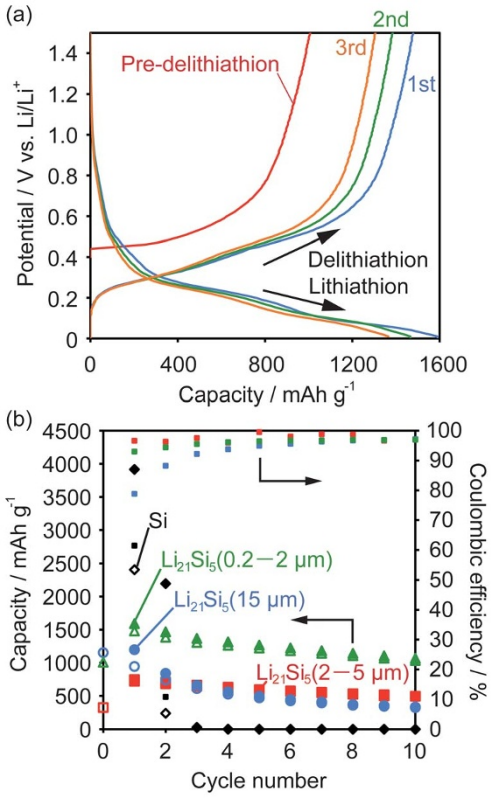

Figure 3 | (a) Charge/discharge curves of $Li_{21}Si_5$(0.2–2 μm) measured at 50 mA g^{-1}. (b) The change of delithiation (open symbol) and lithiation (solid symbol) capacities of Li-Si samples (at 50 mA g^{-1}) and reference Si (10 mA g^{-1}), together with coulombic efficiencies (small solid symbol). Capacity is based on the mass of an active material ($Li_{21}Si_5$ or Si) included in a working electrode.

capacity loss, the obtained pre-delithiation capacity (1007 mAh g^{-1}) is still attractive enough to construct high-energy LIBs by the combination with the lithium-free positive electrodes (Fig. 1). In the subsequent lithiation process (1st lithiation in Fig. 3a), a high capacity of 1591 mAh g^{-1} is obtained, which is higher than the pre-delithiation capacity (1007 mAh g^{-1}), suggesting that some amount of Li was already lost from $Li_{21}Si_5$(0.2–2 μm) before the initial pre-delithiation, as described before. The resulting lithiation capacity (1591 mAh g^{-1}) corresponds to 81% of the theoretical capacity of $Li_{21}Si_5$, being much higher than the values of Li-Si alloys in the literatures (300 to 800 mAh g^{-1})[33–35,37]. Thus, the present measurement setup reveals that Li-rich Li-Si alloy possesses an attractive potential as a high-capacity negative electrode material.

Fig. 3b shows capacity change of the Li-Si alloys for 10 charge/discharge cycles. The 1st lithiation and delithiation capacities of $Li_{21}Si_5$(0.2–2 μm) are 1591 and 1480 mAh g^{-1}, respectively. The 1st coulombic efficiency is thus 93%, and it increases with cycle number. At the 10th cycle, this sample still retains a high lithiation capacity of 1067 mAh g^{-1}. It is noteworthy that the lithiation/delithiation curves after the pre-delithiation (Fig. 3a) are very similar to those of amorphous Si[39]. Such similarity is more clearly seen in the differential capacity plots of Fig. 3a (Supporting Information, Fig. S1). This finding suggests that electrochemically active Li-Si alloy embedded in the Cu pellet is delithiated and then transformed into amorphous Si, and after the pre-delithiation, the amorphous Si thus formed can be charged/discharged with showing a high capacity.

To investigate the effect of particle size, the as-synthesized Li-Si alloy was simply crushed with a pestle in a mortar, and the sample with a larger particle size (approximately 15 μm, measured by SEM) was prepared. This sample is referred to as $Li_{21}Si_5$(15 μm), and its charge/discharge capacities were also examined. The results are shown in Fig. 3b. It shows a high pre-delithiation capacity of 1153 mAh g^{-1}, probably because this sample is free from the delithiation by the severe ball-milling process. However, its cycle performance is worse than that of $Li_{21}Si_5$(0.2–2 μm): the high 1st lithiation capacity (1198 mAh g^{-1}) of $Li_{21}Si_5$(15 μm) fades to 316 mAh g^{-1} in the 10th cycle. By crushing Li-Si alloy into powder having a particle size of 2–5 μm, the cyclability is a little improved as shown in Fig. 3b: the 1st and the 10th lithiation capacities are 747 and 494 mAh g^{-1}, respectively, in $Li_{21}Si_5$(2–5 μm). By making the particle size 0.2–2 μm, the capacity and cyclability is remarkably improved. Thus, smaller particle size is preferable in Li-Si alloy, like the case of Si negative-electrode[39]. This similarity would be due to the fact that Li-Si alloy eventually turns into amorphous Si after the pre-delithiation. In the case of Si, its capacity, rate performance, and cyclability can be improved when the domain size is smaller than about 1 μm, and the performance becomes much better with decreasing the domain size down to tens of nanometers[14,39–46].

The structure change of the Li-Si alloy during charge/discharge is very much different from that of Si. To elucidate such difference, charge/discharge behaviors of Si powder (particle size is less than 2 μm) were also examined in the same manner as in the case of the Li-Si alloy, and the charge/discharge capacities of Si are shown in Fig. 3b. Note that the volume fraction of Si/Cu was adjusted to the same as that of Li-Si/Cu when a pellet for a working electrode was prepared. Though Si shows a very high initial lithiation capacity up to 3916 mAh g^{-1} (based on the Si weight), its capacity fades very quickly and is almost lost as early as the 3rd cycle. This is because of the intense volume expansion of Si up to about 3–4 times larger than the original Si volume upon the lithiation[47]. Such volume expansion aggressively destroys the Cu support, thereby giving rise to the electrical isolation of the lithiated Si and the quick loss of its capacity as a result. To confirm the bulk structure change of the Si/Cu pellet electrode, the three-electrode cell was dismantled after 10 charge/discharge cycles, and it was found that the pellet completely collapsed into powder. By contrast, the bulk structure of the $Li_{21}Si_5$(2–5 μm)/Cu pellet electrode was unchanged after 10 charge/discharge cycles, since Li-Si alloy has been already lithiated and its volume does not expand.

Microstructures of Li-Si/Cu electrode before and after 10 charge/discharge cycling are directly observed by SEM equipped with an energy dispersive X-ray spectrometer (EDX). Fig. 4a shows a cross-sectional SEM image of the pellet electrode prepared from $Li_{21}Si_5$(2–5 μm) and Cu powder before the electrochemical measurements. The positions of Li-Si alloy and Cu can be identified from the elemental mappings for Si (Fig. 4b) and Cu (Fig. 4c), respectively. In Fig. 4a, Li-Si particles, which are indicated by arrows, have relatively smooth surface. The other particles with rather wrinkled appearance must be Cu, as found from Fig. 4c. Li-Si alloy and Cu particles are homogeneously mixed and they are closely packed in the pellet electrode. Fig. 4d shows a SEM image of the pellet electrode after the 10th delithiation, and the positions of Si and Cu are confirmed by Fig. 4e and f, respectively. Also in Fig. 4d, Si particles are clearly identified as indicated by arrows from the Cu matrix. It is noteworthy that the size and the shape of the Si particles (Fig. 4d) after 10 cycles are almost the same as those of the original Li-Si particles (Fig. 4a). Such similarities in morphology seem a little strange, when considering the very different densities of $Li_{21}Si_5$ (1.18 g cm^{-3}) and Si (2.33 g cm^{-3}). In order to elucidate this result, the electrodes shown in Fig. 4a and d are further observed by a transmission electron microscope (TEM) and selected area electron diffraction (SAD) equipped with EDX, as shown in Fig. 4g and h. Note that we confirmed the absence of Cu in the viewing fields of Fig. 4g and h by EDX. From the change of the SAD pattern, it is found that polycrystalline Li-Si alloy, which is assigned as $Li_{21}Si_5$ or $Li_{17}Si_4$ (Fig. 4g), is turned into amorphous Si (Fig. 4h) by the charge/discharge cycling, as we have already presumed. In addition, the original dense structure of Li-Si alloy (Fig. 4g) is changed into an aggregation of very small particles (Fig. 4h), indicating that the amorphous Si has a sponge-like porous structure and the density of the particles shown in Fig. 4d is actually much lower than that of crystalline Si (2.33 g cm^{-3}) due to its inner porosity. N_2 adsorption isotherm of the sponge-like porous Si after the delithiation (Fig. 4i) indeed shows adsorption uptake above $P/P_0 = 0.8$, which corresponds to the presence of large mesopores/macropores in this sample. With becoming porous structure, surface decomposition of the electrolyte becomes intense, and thus, Li-Si alloy shares the same problem with a Si anode, which also increases its surface area during charge/discharge cycling[39]. It is therefore important to suppress/delay the evolution of porosity. The carbon-coating of Li-Si alloy and/or the restriction of upper-limit capacity may be effective, like the case of Si[39]. Another method is the use of effective additives of electrolyte[48].

The structure change of the Li-Si/Cu pellet upon its delithiation/lithiation can be illustrated as Fig. 5a. In the first delithiation step, Li-Si particles become porous Si. In the subsequent lithiation step, the porous Si particles would turn into dense Li-Si alloy, but their particle sizes do not exceed the original sizes of Li-Si alloy. Then, lithiation/delithiation could be repeated in the following cycles without the destruction of Cu-supporting electrode disc. The transformation of Li-Si alloy into the sponge-like porous Si would be one of the essential reasons for the better cyclability, since the presence of pores around Si framework can buffer the stress generated by the expansion of Si upon lithiation. On the other hand, the Si particles significantly expand up to about 3–4 times larger than their original sizes especially upon the first lithiation and the Cu-supporting electrode disc is therefore totally destroyed (Fig. 5b).

We then examine the feasibility of the Li-rich Li-Si alloy as a Li-containing negative electrode by combining it with a Li-free positive electrode. Commercially available MnO_2 powder was used as the latter. Before constructing a full cell, charge/discharge behavior of MnO_2 is examined with a half cell, as shown in Fig. 6a. Although MnO_2 shows a relatively large irreversible capacity of 119 mAh g^{-1}

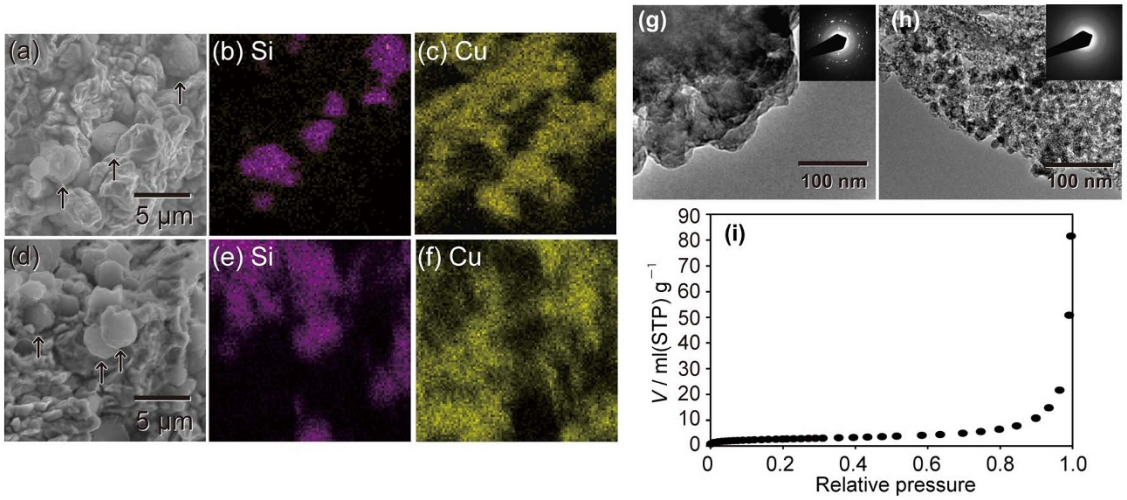

Figure 4 | (a,d) SEM images and (b,c,e,f) elemental mappings for Si and Cu at the cross-section of $Li_{21}Si_5$(2–5 μm)/Cu electrodes (a–c) before charge/discharge measurements and (d–f) after 10 cycles (after delithiation). The positions of Li-Si alloy or Si are indicated by arrows. (g,h) TEM images of $Li_{21}Si_5$(2–5 μm) (g) before and (h) after charge/discharge measurements. Insets represent SAD patterns. (i) N_2 adsorption isotherm (−196°C) of porous Si shown in (h).

in the 1st cycle, those in the 2nd and the 3rd cycles are reduced down to ca. 20 mAh g^{-1}. Its 2nd and 3rd lithiation capacities are 140 and 132 mAh g^{-1}, respectively. Next, a full cell was constructed by using $Li_{21}Si_5$(0.2–2 μm) and MnO_2 as negative and positive electrodes, respectively. Fig. 6b shows its charge/discharge curves. Note that the amount of MnO_2 is ca. 3 times larger than that of $Li_{21}Si_5$(0.2–2 μm) to balance the Li storage capacities in negative and positive electrodes. The full cell shows the 1st discharge and charge capacities of 479 and 304 mAh g^{-1}, respectively. The first irreversible capacity is relatively high (175 mAh g^{-1}). This is mainly due to the irreversible capacity of MnO_2, as shown in Fig. 6a. Based on the pre-delithiation capacities of $Li_{21}Si_5$(0.2–2 μm) (Fig. 3a) and the 1st charge/discharge capacity of MnO_2 (Fig. 6a) as well as their amounts in each of the electrodes, the 1st discharge/charge capacities of the full cell is estimated as 745/349 mAh g^{-1}-$Li_{21}Si_5$. Note that the large difference between discharge and charge capacities is due to the large irreversible capacity of MnO_2. The reason why the actual capacities are lower than the estimation would be the different potential profiles between half cells (Fig. 3a and 6a) and the full cell (Fig. 6b) in each of electrodes. By the same way, the 2nd discharge/charge capacities are also estimated as 466/389 mAh g^{-1}-$Li_{21}Si_5$, while the actual values are 331/300 mAh g^{-1}-$Li_{21}Si_5$. The full cell shows almost reasonable capacities. In order to evaluate the validity of the Li-rich Li-Si alloy as a lithium-containing negative electrode, we carried out a comparative experiment by using pre-lithiated graphite (LiC_6), which is popularly used as a lithium-containing negative electrode in lithium-ion capacitors, and is expected as another candidate of a counter material of sulfur electrode (Fig. 1). Its charge/discharge curves are shown in Fig. 6c. Due to the smaller capacity of the pre-lithiated graphite (339 mAh g^{-1}-LiC_6), its full-cell shows much lower capacity than the case of $Li_{21}Si_5$(0.2–2 μm) (Fig. 6b), clearly indicating the advantage of the Li-rich Li-Si alloy as a promising lithium-containing negative electrode for next-generation high-energy LIBs.

The Cu-supported pellet electrode used in the above discussion contains a very small amount of Li-Si alloy (ca. 5 wt%), and it is too heavy for practical LIBs. Therefore, we prepare a lighter electrode sheet, which is of importance for practical use, by mixing $Li_{21}Si_5$(0.2–2 μm) with two types of carbon blacks (CBs; conductive additive) and PTFE (binder polymer). Since Li-Si alloy severely reacts with PTFE, the surface of Li-Si particles was first covered with CBs (their SEM images are shown in Fig. S2) simply by their physical mixing. After the coating, the original smooth appearance of a $Li_{21}Si_5$(0.2–2 μm) particle (Fig. S3a) turns to be noticeably rough (Fig. S3b), due to the presence of CBs on the whole surface of the $Li_{21}Si_5$(0.2–2 μm) particle. The resulting carbon-coated Li-Si alloy was able to be mixed with PTFE without any reactions and the content of $Li_{21}Si_5$(0.2–2 μm) in the obtained sheet is 53 wt%, which is much higher than the case of the Cu-supported pellet (5 wt%).

Fig. 7a shows the lithiation/delithiation capacities of a half-cell including the sheet electrode at 50 mA g^{-1}. For comparison, the data of the Cu pellet electrode consisting of $Li_{21}Si_5$(0.2–2 μm) are also plotted. The pre-delithiation capacity of $Li_{21}Si_5$(0.2–2 μm) in the sheet electrode is 1219 mAh g^{-1}, which is higher than the case of the Cu pellet electrode. Such high pre-delithiation capacity suggests that Li-Si alloy does not react with PTFE owing to the carbon-coating. The 1st lithiation/delithiation capacities are 1598/1457 mAh g^{-1}, almost the same as the case of the Cu pellet electrode. In addition, the 10th lithiation/delithiation capacities (1220/1179 mAh g^{-1}) are higher than those in the pellet electrode. Thus, $Li_{21}Si_5$(0.2–2 μm) embedded in the sheet electrode exhibits no less performance than the case of the Cu pellet electrode. Fig. 7b compares the capacities of these two electrodes, based on the weight of the total electrode weight. By preparing the lighter sheet electrode, the capacity based on the whole electrode weight can be greatly increased. Thus, carbon-

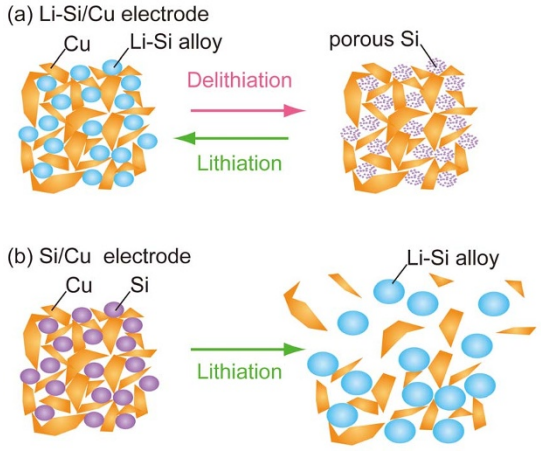

Figure 5 | **Illustrations for the structure change of (a) Li-Si/Cu and (b) Si/Cu electrodes by delithiation and/or lithiation.**

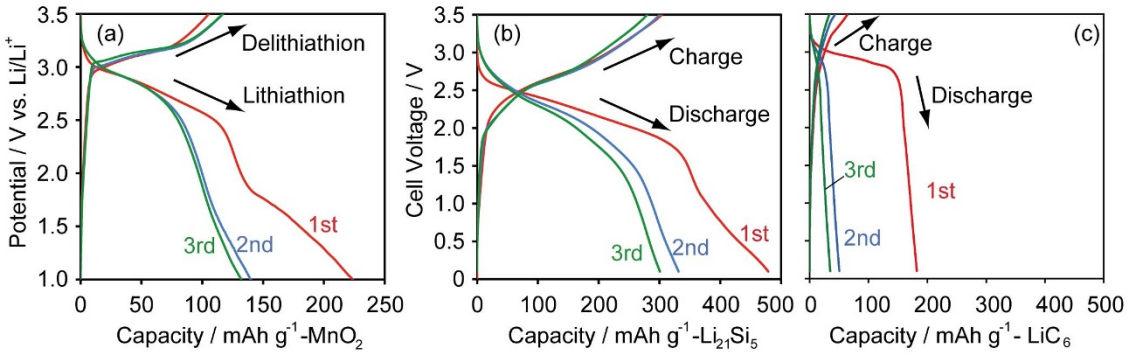

Figure 6 | Charge/discharge curves of (a) a half-cell of MnO_2 and full-cells constructed with (b) MnO_2/$Li_{21}Si_5$(0.2–2 μm) and (c) MnO_2/pre-lithiated graphite at 10 mA g^{-1}.

coating is an effective way to avoid undesirable reactions between Li-Si alloy and the binder polymer, and would be crucial to utilize Li-rich Li-Si alloy as a lithium-containing negative electrode. This work has revealed the promising potential of Li-rich Li-Si alloy and demonstrated the method to prepare a light electrode sheet, based on the data obtained at early stage of charge/discharge. To achieve a long cycling life and to make the Li-Si alloy more practical, further improvement must be necessary, such as optimization of particle size, formation of composites with carbon, and/or appropriate surface oxidation[38]. We hope that this work could be a starting point of such future works.

Conclusions

The potential of Li-rich Li-Si alloy having the composition of $Li_{21}Si_5$ as a Li-containing negative electrode for LIBs is examined in detail. Decreasing particle size is effective to improve its performance. Li-Si alloy shows a high initial lithium-extraction capacity of 1000 mAh g^{-1}, which is attractive enough to construct high-energy LIBs by the combination with the lithium-free positive electrode materials, such as sulfur. It is suggested that crystalline Li-Si alloy turns into porous and amorphous Si upon delithiation, and then the amorphous Si turns into amorphous Li-Si alloy upon the subsequent lithiation. Interestingly, the original particle size of Li-Si alloy is almost unchanged even by several charge/discharge cycles. Since the present Li-Si alloy is free from severe volume change unlike Si, the cyclability of Li-Si alloy is much better than Si. In addition, we have successfully demonstrated the charge/discharge of a prototype LIB cell consisting of Li-Si alloy as a lithium-containing negative electrode, together with a lithium-free positive electrode, and the cell capacity is much higher than another test LIB cell with pre-lithiated graphite instead of Li-Si alloy. Though Li-rich Li-Si alloy is too active to be mixed with binder polymers for the preparation of conventional sheet electrodes, the coating with carbon black powder is found to prevent the undesirable reactions of Li-Si alloy with binder polymers. The present results demonstrate a promising potential of Li-rich Li-Si alloy as a counter part of a high-capacity lithium-free positive electrode materials, towards ultrahigh-energy LIBs.

Methods

Preparation of Li-Si alloy. Li (99.9%, Honjo Metal Co., Ltd.) and Si powder (99,9%, particle size: 1 ~ 2 μm, Soekawa Chemical Co., Ltd.) were taken with a molar ratio of 21 : 5 (total mass is about 2 g), and they were put into a tantalum vessel and they were packed inside a closed vessel of stainless steel (SUS316) in an argon-filled glove-box. The tightly sealed vessel was heated at 750°C for 1 h in a muffle furnace (Denken-highdental Co., Ltd., KFD-S90) to melt the mixture, and then the vessel was cooled down to complete a solidification of Li-Si alloy having the composition of $Li_{21}Si_5$. The Li-Si alloy thus obtained was crushed into a fine powder with a planet ball mill (Fritsch, premium line P-7) under Ar atmosphere. Two different conditions were performed: a low-speed milling at 750 rpm for 720 min using agate balls (10 mm) in an agate vessel, and a high-speed milling at 1100 rpm for 120 min using zirconium beads (1 mm) in a zirconium vessel. The former is softer, while the latter is harder, and they yielded fine powders with the particle sizes of ca. 2–5 μm and 0.2–2 μm, respectively. The resulting samples are referred to as $Li_{21}Si_5$(2–5 μm) and $Li_{21}Si_5$(0.2–2 μm), respectively.

Characterization. Powder XRD patterns were measured for as-synthesized Li-Si alloy and its crushed powder with a Shimadzu XRD-6100 diffractometer with Cu Kα radiation generated at 30 kV and 20 mA. The sample was set in a home-made sealed sample holder to avoid the exposure of the sample to air. The sample holder is equipped with an X-ray permeable window made by a polyimide film. The ball-milled Li-Si powders were observed with SEM (Hitachi, S-4800), by using a home-made transfer vessel which enables to transfer the sample from Ar-filled glove-box to a chamber of SEM without exposure of the sample to air.

Charge/discharge measurements of Li-Si alloy with a half-cell. Li-Si powder and Cu powder (Aldrich) were mixed at the ratio of 5 : 95 by weight (29 : 71 by volume) and they were pressed into a pellet with a diameter and a thickness of 12 mm and 200 μm, respectively. About 10 mg of Li-Si alloy was included in the pellet. For comparison, a

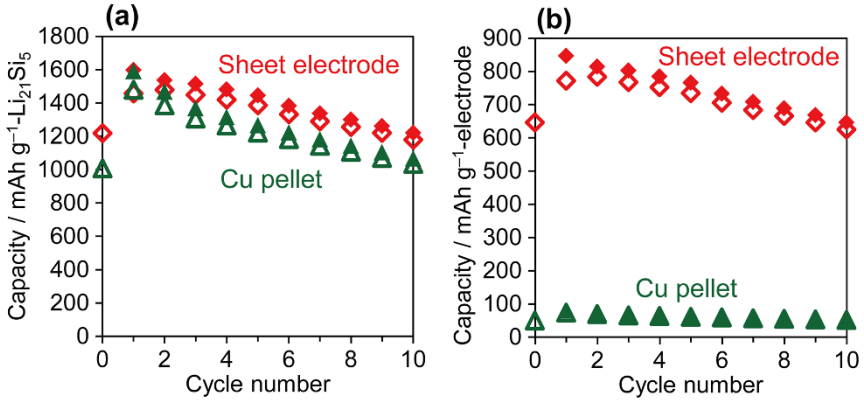

Figure 7 | The change of delithiation (open symbol) and lithiation (solid symbol) capacities of $Li_{21}Si_5$(0.2–2 μm) included in the Cu-pellet electrode or a sheet electrode. Current density is 50 mA g^{-1}. Capacity is calculated based on (a) $Li_{21}Si_5$ and (b) the total electrode weight, respectively.

similar pellet electrode was prepared by using Si instead of Li-Si. In this case, the volume ratio of Si was adjusted to be the same as the case of Li-Si, i.e., the ratio of Si : Cu was 29 : 71 by volume. The pellet electrode was packed into a three electrode cell together with a polypropylene separator. Two pieces of lithium foil were used as a counter and a reference electrodes. An electrolyte solution was 1 M $LiPF_6$ in a mixture of ethylene carbonate and diethyl carbonate (1 : 1 by volume). The three-electrode cell was galvanostatically charged/discharged at the range of 0.01–1.5 V vs. Li/Li^+ and the current density of 50 mA g^{-1}. All the measurements were carried out at 25°C. The pellet electrode including Li-Si was observed before and after charge/discharge measurement by SEM equipped with EDX (EDAX inc., Genesis XM2M). Also in this case, the aforementioned transfer vessel was used. Li-Si electrode before and after charge/discharge cycling was observed also by TEM (TEM; JEOL, JEM-2010) together with SAD equipped with EDX (Noran Voyger). Nitrogen adsorption property of an electrode pellet prepared by $Li_{21}Si_5$(2–5 μm) after 10 cycles was measured with a volumetric sorption analyzer (BELSORP MINI II, BEL Japan) at −196°C after washing with DEC and drying at 150°C for 6 h under vacuuming. Then, the nitrogen adsorption amount in the delithiated Si was calculated based of the weight ratio of Si atoms which is contained in the electrode pellet at the ratio of 2.5 wt%. Note that the porosity of Cu pellet is not detected by the nitrogen adsorption measurement, since the pore size is in the range of micrometers.

Charge/discharge measurement of MnO_2 with a half-cell. MnO_2 was characterized by a half cell. MnO_2 powder (Tosoh co.) was mixed with a binder polymer solution (12 wt% poly(vinylidene fluoride) (PVDF) dissolved in *N*-methyl-2-pyrrolidone) and acetylene black (AB; Denka black, Denki kagaku kogyo), and the resulting slurry was pasted onto a copper foil. After dried at 80°C in air for 1 h, the film was cut into a circular shape (16 mm in diameter). The weight ratio of MnO_2, AB and PVDF was 8 : 1 : 1, and the amount of MnO_2 in the electrode was ca. 16 mg. Then, the electrode was assembled into a half cell together with the Li counter/reference. The half-cell was galvanostatically charged/discharged at 10 mA g^{-1}-MnO_2 in a potential range between 1.0–3.5 V vs. Li/Li^+.

Charge/discharge measurement with a full-cell. A full-cell was prepared by using $Li_{21}Si_5$(0.2–2 μm) and MnO_2 as negative and positive electrodes, respectively. Note that the thickness of a $Li_{21}Si_5$(0.2–2 μm)/Cu pellet electrode in this case is one half of that for the half-cell. About 5 mg of $Li_{21}Si_5$(0.2–2 μm) was included in the pellet. The full-cell was galvanostatically charged/discharged at 10 mA g^{-1}-$Li_{21}Si_5$ in the cell voltage between 0.1–3.5 V. Pre-lithiated graphite is prepared by the electrochemical pre-doping of lithium. First, graphite electrode was prepared from graphite powder (Nippon steel & sumikin chemical co., LTD.; natural graphite) and PVDF at the weight ratio of 9 : 1. They were coated on a copper foil by the same method as the MnO_2 electrode. The amount of graphite in an electrode was ca. 3 mg, which is the same as Si amount in $Li_{21}Si_5$(0.2–2 μm) electrode. The graphite electrode was galvanostatically pre-lithiated in a half-cell at 50 mA g^{-1} up to 350 mAh g^{-1}. After lithiation, the pre-lithiated graphite electrode was taken out and put into a full-cell together with a MnO_2 counter electrode. The full-cell was galvanostatically charged/discharged at 10 mA g^{-1}-graphite in the cell voltage between 0.1–3.5 V.

Charge/discharge measurement with a half-cell by a PTFE electrode. $Li_{21}Si_5$(0.2–2 μm) was coated with CBs, which is a mixture of AB and ketjen black (EC600JD; Lion) at the rate of 3 : 1, by physical mixing using a ball-milling apparatus (Asahi-rika co., AV-01) at 60 rpm for 60 min using agate balls (1 mm) in glass vessel. Carbon-coated $Li_{21}Si_5$(0.2–2 μm) powder was kneaded with PTFE (Dupont) and additional AB in an agate mortar until becoming a homogeneous paste. The paste was shaped into a circular disk and pushed on a Cu mesh (Nilaco Co.; 100 mesh) to make a working electrode. The weight ratio of $Li_{21}Si_5$(0.2–2 μm)/PTFE/CBs in the electrode was 53/26/21 and the amount of $Li_{21}Si_5$(0.2–2 μm) was ca. 4 mg. Then, the electrode was assembled into a half cell together with the Li counter/reference. The half-cell was galvanostatically charged/discharged at 50 mA g^{-1}-$Li_{21}Si_5$ in a potential range between 0.1–1.5 V.

1. Tarascon, J. M. & Armand, M. Issues and challenges facing rechargeable lithium batteries. *Nature* **414**, 359–367; DOI:10.1038/35104644 (2001).
2. Arico, A. S., Bruce, P., Scrosati, B., Tarascon, J. M. & Van Schalkwijk, W. Nanostructured materials for advanced energy conversion and storage devices. *Nat. Mater* **4**, 366–377; DOI:10.1038/nmat1368 (2005).
3. Lee, S. Y. *et al.* Progress in flexible energy storage and conversion systems, with a focus on cable-type lithium-ion batteries. *Energy Environ. Sci* **6**, 2414–2423; DOI:10.1039/c3ee24260a (2013).
4. Nishihara, H. & Kyotani, T. Templated nanocarbons for energy storage. *Adv. Mater* **24**, 4473–4498; DOI:10.1002/adma.201201715 (2012).
5. Obrovac, M. N. & Christensen, L. Structural changes in silicon anodes during lithium insertion/extraction. *Electrochem. Solid State Lett* **7**, A93–A96; DOI:10.1149/1.1652421 (2004).
6. Hatchard, T. D. & Dahn, J. R. In situ XRD and electrochemical study of the reaction of lithium with amorphous silicon. *J. Electrochem. Soc* **151**, A838–A842; DOI:10.1149/1.1739217 (2004).
7. Cui, L. F., Yang, Y., Hsu, C. M. & Cui, Y. Carbon-silicon core-shell nanowires as high capacity electrode for lithium ion batteries. *Nano Lett* **9**, 3370–3374; DOI:10.1021/nl901670t (2009).
8. Song, T. *et al.* Arrays of sealed silicon nanotubes as anodes for lithium ion batteries. *Nano Lett* **10**, 1710–1716; DOI:10.1021/nl100086e (2010).
9. Chen, X. L. *et al.* A patterned 3D silicon anode fabricated by electrodeposition on a virus-structured current collector. *Adv. Funct. Mater* **21**, 380–387; DOI:10.1002/adfm.201001475 (2011).
10. Chan, C. K. *et al.* High-performance lithium battery anodes using silicon nanowires. *Nat. Nanotechnol* **3**, 31–35; DOI:10.1038/nnano.2007.411 (2008).
11. Kim, H. & Cho, J. Superior lithium electroactive mesoporous Si@carbon core-shell nanowires for lithium battery anode material. *Nano Lett* **8**, 3688–3691; DOI:10.1021/nl801853x (2008).
12. Magasinski, A. *et al.* High-performance lithium-ion anodes using a hierarchical bottom-up approach. *Nat. Mater* **9**, 353–358; DOI:10.1038/nmat2725 (2010).
13. Kovalenko, I. *et al.* A major constituent of brown algae for use in high-capacity Li-ion batteries. *Science* **333**, 75–79; DOI:10.1126/science.1209150 (2011).
14. Kim, H., Seo, M., Park, M. H. & Cho, J. A critical size of silicon nano-anodes for lithium rechargeable batteries. *Angew. Chem. Int. Ed* **49**, 2146–2149; DOI:10.1002/anie.200906287 (2010).
15. Hasegawa, T., Mukai, S. R., Shirato, Y. & Tamon, H. Preparation of carbon gel microspheres containing silicon powder for lithium ion battery anodes. *Carbon* **42**, 2573–2579; DOI:10.1016/j.carbon.2004.05.050 (2004).
16. Chae, C., Noh, H. J., Lee, J. K., Scrosati, B. & Sun, Y. K. A high-energy Li-ion battery using a silicon-based anode and a nano-structured layered composite cathode. *Adv. Funct. Mater* **24**, 3036–3042; DOI:10.1002/adfm.201303766 (2014).
17. Lee, J. I., Park, J. H., Lee, S. Y. & Park, S. Surface engineering of sponge-like silicon particles for high-performance lithium-ion battery anodes. *Phys. Chem. Chem. Phys* **15**, 7045–7049; DOI:10.1039/c3cp51190a (2013).
18. Bogart, T. D. *et al.* Lithium ion battery peformance of silicon nanowires with carbon skin. *ACS Nano* **8**, 915–922; DOI:10.1021/nn405710w (2014).
19. Murugesan, S., Harris, J. T., Korgel, B. A. & Stevenson, K. J. Copper-coated amorphous silicon particles as an anode material for lithium-ion batteries. *Chem. Mater* **24**, 1306–1315; DOI:10.1021/cm2037475 (2012).
20. Chockla, A. M., Klavetter, K. C., Mullins, C. B. & Korgel, B. A. Tin-seeded silicon nanowires for high capacity Li-ion batteries. *Chem. Mater* **24**, 3738–3745; DOI:10.1021/cm301968b (2012).
21. Kasavajjula, U., Wang, C. S. & Appleby, A. J. Nano- and bulk-silicon-based insertion anodes for lithium-ion secondary cells. *J. Power Sources* **163**, 1003–1039; DOI:10.1016/j.jpowsour.2006.09.084 (2007).
22. Whittingham, M. S. Lithium batteries and cathode materials. *Chem. Rev* **104**, 4271–4301; DOI:10.1021/cr020731c (2004).
23. Li, B. H. *et al.* Facile synthesis of $Li_4Ti_5O_{12}$/C composite with super rate performance. *Energy Environ. Sci* **5**, 9595–9602; DOI:10.1039/c2ee22591c (2012).
24. Badway, F., Cosandey, F., Pereira, N. & Amatucci, G. G. Carbon metal fluoride nanocomposites - High-capacity reversible metal fluoride conversion materials as rechargeable positive electrodes for Li batteries. *J. Electrochem. Soc* **150**, A1318–A1327; DOI:10.1149/1.1602454 (2003).
25. Ji, X. L. & Nazar, L. F. Advances in Li-S batteries. *J. Mater. Chem* **20**, 9821–9826; DOI:10.1039/b925751a (2010).
26. Huang, J. Q. *et al.* Aligned sulfur-coated carbon nanotubes with a polyethylene glycol barrier at one end for use as a high efficiency sulfur cathode. *Carbon* **58**, 99–106; DOI:10.1016/j.carbon.2013.02.037 (2013).
27. Huang, J. Q. *et al.* Entrapment of sulfur in hierarchical porous graphene for lithium-sulfur batteries with high rate performance from-40 to 60 degrees C. *Nano Energy* **2**, 314–321; DOI:10.1016/j.nanoen.2012.10.003 (2013).
28. JM Energy Corporation, *Feature of LIC*, Available at: http://www.jmenergy.co.jp/en/product_whats.html. (Accessed: 25th October 2014).
29. Vandermarel, C., Vinke, G. J. B. & Vanderlugt, W. The phase-diagram of the system lithium-silicon. *Solid State Communications* **54**, 917–919; DOI:10.1016/0038-1098(85)90155-3 (1985).
30. Nesper, R. & Vonschnering, H. G. Li_2Si_5, a zintl phase as well as a Hume-Rothery phase. *J. Solid State Chem* **70**, 48–57; DOI:10.1016/0022-4596(87)90176-9 (1987).
31. Zeilinger, M., Benson, D., Haussermann, U. & Fassler, T. F. Single crystal growth and thermodynamic stability of $Li_{17}Si_4$. *Chem. Mater* **25**, 1960–1967; DOI:10.1021/cm400612k (2013).
32. Szczech, J. R. & Jin, S. Nanostructured silicon for high capacity lithium battery anodes. *Energy Environ. Sci* **4**, 56–72; DOI:10.1039/c0ee00281j (2011).
33. Weydanz, W. J., Wohlfahrt-Mehrens, M. & Huggins, R. A. A room temperature study of the binary lithium-silicon and the ternary lithium-chromium-silicon system for use in rechargeable lithium batteries. *J. Power Sources* **81**, 237–242; DOI:10.1016/s0378-7753(99)00139-1 (1999).
34. Tamori, R., Machida, N. & Shigematsu, T. Preparation of $Li_{4.4}Si$ alloy by use of mechanical milling methods and its properties as negative electrodes in lithium cells. *J. Jpn. Soc. Powder Powder Metall* **48**, 267–273 (2001).
35. Hashimoto, Y., Machida, N. & Shigematsu, T. Preparation of $Li_{4.4}Ge_xSi_{1-x}$ alloys by mechanical milling process and their properties as anode materials in all-solid-state lithium batteries. *Solid State Ionics* **175**, 177–180; DOI:10.1016/j.ssi.2004.08.022 (2004).
36. Ma, R. J., Liu, Y. F., He, Y. P., Gao, M. X. & Pan, H. G. Chemical preinsertion of lithium: An approach to improve the intrinsic capacity retention of bulk Si anodes for Li-ion batteries. *J. Phys. Chem. Lett* **3**, 3555–3558; DOI:10.1021/jz301762x (2012).

37. Tang, W. S., Chotard, J. N. & Janotz, R. Synthesis of single-phase LiSi by ball-milling: Electrochemical behavior and hydrogenation properties. *J. Electrochem. Soc* **160**, A1232–A1240; DOI:10.1149/2.089308jes (2013).
38. Zhao, J., Lu, Z., Liu, N., Lee, H. W., McDowell, M. T. & Cui, Y. Dry-air-stable lithium silicide-lithium oxide core-shell nanoparticles as high-capacity prelithiation reagents. *Nat. Commun* **5**, 5088, DOI:10.1038/ncomms6088 (2014).
39. Iwamura, S., Nishihara, H. & Kyotani, T. Fast and reversible lithium storage in a wrinkled structure formed from Si nanoparticles during lithiation/delithiation cycling. *J. Power Sources* **222**, 400–409; DOI:10.1016/j.jpowsour.2012.09.003 (2013).
40. Ding, N. *et al.* Determination of the diffusion coefficient of lithium ions in nano-Si. *Solid State Ionics* **180**, 222–225; DOI:10.1016/j.ssi.2008.12.015 (2009).
41. Graetz, J., Ahn, C. C., Yazami, R. & Fultz, B. Highly reversible lithium storage in nanostructured silicon. *Electrochem. Solid State Lett* **6**, A194–A197; DOI:10.1149/1.1596917 (2003).
42. Gauthier, M. *et al.* A low-cost and high performance ball-milled Si-based negative electrode for high-energy Li-ion batteries. *Energy Environ. Sci* **6**, 2145–2155; DOI:10.1039/c3ee41318g (2013).
43. Gohier, A., Laik, B., Pereira-Ramos, J.-P., Cojocaru, C. S. & Pierre, T.-V. Influence of the diameter distribution on the rate capability of silicon nanowires for lithium-ion batteries. *J. Power Sources* **203**, 135–139; DOI:10.1016/j.jpowsour.2011.12.023 (2012).
44. Saint, J. *et al.* Towards a fundamental understanding of the improved electrochemical performance of silicon-carbon composites. *Adv. Funct. Mater* **17**, 1765–1774; DOI:10.1002/adfm.200600937 (2007).
45. Ryu, I., Choi, J. W., Cui, Y. & Nix, W. D. Size-dependent fracture of Si nanowire battery anodes. *J. Mech. Phys. Solids* **59**, 1717–1730; DOI:10.1016/j.jmps.2011.06.003 (2011).
46. Liu, W. R. *et al.* Effect of electrode structure on performance of Si anode in Li-ion batteries: Si particle size and conductive additive. *J. Power Sources* **140**, 139–144; DOI:10.1016/j.jpowsour.2004.07.032 (2005).
47. Iwamura, S., Nishihara, H. & Kyotani, T. Effect of Buffer Size around Nanosilicon Anode Particles for Lithium-Ion Batteries. *J. Phys. Chem. C* **116**, 6004–6011; DOI:10.1021/jp2093669 (2012).
48. Gauthier, M. *et al.* A low-cost and high performance ball-milled Si-based negative electrode for high-energy Li-ion batteries. *Energy Environ. Sci* **6**, 2145; DOI:10.1039/c3ee41318g (2013).

Acknowledgments

We thank Tosoh co. LTD. and Kureha co. LTD. for kindly supplying MnO_2 and PVDF, respectively. This work was supported partly by JST ALCA program and by Nano-Macro Materials, Devices and System Research Alliance.

Author contributions

This research was planned and overseen by H.T.N. with the advice of H.M., H.Y., H.K.N., T.O. and T.K. The experimental measurements were performed by S.I. and Y.O. Data analysis was performed by S.I., H.T.N. and Y.O. All authors contributed to the manuscript preparation.

Additional information

Supplementary information accompanies this paper at http://www.nature.com/scientificreports

Competing financial interests: The authors declare no competing financial interests.

How to cite this article: Iwamura, S. *et al.* Li-Rich Li-Si Alloy As A Lithium-Containing Negative Electrode Material Towards High Energy Lithium-Ion Batteries. *Sci. Rep.* 5, 8085; DOI:10.1038/srep08085 (2015).